2022

Evaluation Of A Monosynaptic Spinal Circuit In Multiple Mouse Models Of Amyotrophic Lateral Sclerosis

Maura A. Curran
Wright State University

EVALUATION OF A MONOSYNAPTIC SPINAL CIRCUIT IN MULTIPLE MOUSE MODELS OF AMYOTROPHIC LATERAL SCLEROSIS

A Thesis submitted in partial fulfillment of the
requirements for the degree of
Master of Science

by

MAURA A. CURRAN

B.S. Western New England University, 2016

2022

Wright State University

WRIGHT STATE UNIVERSITY

GRADUATE SCHOOL

April 28, 2022

I HEREBY RECOMMEND THAT THE THESIS PREPARED UNDER MY SUPERVISION BY Maura A. Curran ENTITLED Evaluation Of A Monosynaptic Spinal Circuit In Multiple Mouse Models Of Amyotrophic Lateral Sclerosis BE ACCEPTED IN PARTIAL FULFILLMENT OF THE REQUIREMENTS FOR THE DEGREE OF Master of Science

_____

Sherif M. Elbasiouny, Ph.D., PE, P.Eng

Thesis Director

_____

Eric S. Bennett, Ph.D.
Department

Chair Neuroscience, Cell Biology and Physiology

Committee on Final Examination:

_____

Mark Rich, M.D., Ph.D.

_____

David Ladle, Ph.D.

_____

Barry Milligan, Ph.D.

Dean of the Graduate School

ABSTRACT

Curran, Maura A, MS, Department of Neuroscience, Cell Biology and Physiology, Wright State University, 2022. Evaluation Of A Monosynaptic Spinal Circuit In Multiple Mouse Models Of Amyotrophic Lateral Sclerosis

Amyotrophic lateral sclerosis (ALS) is a fatal neurodegenerative disease. To date, there are no significant disease-modifying treatments, and one limiting factor in treatment is the amount of time it takes for a patient to receive a diagnosis of ALS. This study examined multiple mouse models before symptom onset to help identify early changes in a reflex circuit of ALS mice. Dorsal root stimulation of the sacral spinal cord in multiple models ALS mouse models showed changes in the resulting ventral root compound action potential amplitude, latency, and ability to maintain synaptic depression. These data also suggest that a mouse model of TDP43 inclusions is fundamentally different in its network properties than that of SOD1 ALS mutant mice. While these data suggest changes in motor neuron excitability may play a contributing factor, there are likely other synaptic changes involved, but further work needs to be done to verify this.

Table of Contents

List of figures and illustrations

List of Tables

List of Abbreviations

ALS – Amyotrophic Lateral Sclerosis

mACSF – magnesium rich artificial cerebral spinal fluid

nACSF – normal artificial cerebral spinal fluid

P# - denotes postnatal day

SOD1 – Superoxide dismutase 1

TDP43 – TAR DNA binding protein which is 43 kDa

Introduction

Amyotrophic Lateral Sclerosis (ALS) is a severe neurodegenerative disease with a prevalence of about 6/100,000 people (Talbott et al., 2016). The prognosis is three to five years from the time of diagnosis, and while there are two drugs approved for the treatment of ALS, neither offers substantial disease modification (Statland et al., 2015). Riluzole, an inhibitor of excitatory neurotransmission, is the mainstay of treatment as it is the only drug to offer a (small) increase in life expectancy (Bryson et al., 2012). Like with many neurodegenerative diseases, the prevalence of ALS is rising as the general population ages (Arthur et al., 2016). This increases the cost to the healthcare system as many patients develop high care needs before death and emphasizes the importance of improving our understanding of this disorder in the hopes of translating basic science research to better clinical approaches.

One significant limitation to treating ALS in a clinical setting is the length of time from symptom onset to diagnosis. To diagnose ALS, patients must exhibit both upper and lower motor neuron dysfunction, as well as demonstrate the progression of disease over the course of six months (Genç, B. et al. *2017)*. Despite the diagnostic criteria only requiring six months of progression, it takes sporadic disease patients a median of eleven months from symptom onset to receive a diagnosis (Paganoni et al. 2015). This delay is largely due to the heterogeneous and nonspecific initial presentation of the disease. This diagnostic delay, however, presents a problem. By the time weakness can be measured clinically, the motor neuron pool may be diminished by as much as 50-80% (de Carvalho and Swash, 2016). As the delay for diagnosis continues (and thus further disease progression), there is further motor neuron loss which is then irreversible. This problem limits the potential benefit of any disease-modifying treatment

and creates the need to better understand changes that occur early in the disease state in order to develop better diagnostic methods.

Despite a significant need to better understand early changes in the disease, the pathogenesis of ALS is still widely debated, because it is likely multifactorial. It is hypothesized that ALS begins with motor neuron excitability. However, it is still debated as to whether it starts with upper or lower motor neuron hyperexcitability (van den Bos and Medhi, 2019). It is believed that this hyperexcitability leads to increased intracellular calcium and thus cell death, a process known as excitotoxicity. There is evidence for several mechanisms contributing to this excitotoxicity, from direct causes such as increased extracellular glutamate to indirect causes such as decreased inhibition, alterations in glutamate receptors, and increased intrinsic motor neuron excitability (reviewed in King et al. 2016). Additionally, many of the known genetic causes of ALS affect pathways having to do with the response to cell stress, and so an increased vulnerability to excitotoxicity also likely plays a role (Ludolph et al., 2000).

In addition to the delay in diagnostic time, there is no way to adequately predict who will develop ALS because 90% of patients have a sporadic form of the disease rather than a familial form (Kurland and Mulder, 1955). Genetic disease, however, is most useful for research purposes as animal models can be made to replicate human disease and thus can be tested for the genetic variants long before symptom onset allowing researchers to study disease changes that occur long before a human patient would present to the clinic. Of the 10% of patients with familial ALS, approximately 20% of those have a mutation in the superoxide dismutase (SOD1) protein, which helps limit free radical cell toxicity (Rosen et al., 1993). Another important mutation to note includes those in the TAR DNA binding protein (about 5% of familial cases), which leads to intracellular accumulations, which interestingly are found in 97% of ALS patients despite mutation status (Da Cruz and Cleaveland, 2011). Other mutations include those in

C90RF72, which accounts for about 40% of familial ALS cases but whose function is still unknown, and FUS which is a RNA binding protein and accounts for about 4% of familial ALS cases (Boylan, 2015).

The high percentage of familial ALS patients with SOD1 mutations, as well as it being the first mutation to be discovered has led to the development of mouse models with overexpression of mutated SOD1, which are the most used mouse models in ALS research. These mouse models are well characterized and contributed to the development of riluzole (Gurney et al., 1994; Bryson et al., 2012). They also have created the opportunity to study changes in motor neuron pathology long before the onset of disease. The high copy SOD1 model, which has greater than 25 copies of SOD1 human transgene, begins to show changes as early as ten days after birth (P10). The cell size for SOD1 motor neurons is larger than their wild-type littermates (Dukkipati et al., 2018), and electrophysiology experiments have shown an increase in cell excitability (van Dundert et al., 2008; Quinlin et al., 2011; Leroy et al., 2014). Motor neuron damage has been reported as early as 30 days after birth (Hegedus et al., 2007); however, symptom onset does not occur until approximately 90 days after birth (Gurney et al., 1994). While there are significant limitations to testing for changes prior to the time of diagnosis in humans, there is some evidence from retrospective patient analyses that early subclinical changes may occur, indicating some extent of neurodegeneration long before the disease can be clinically diagnosed (Swash and Ingram, 1988). This means the early changes in mice may also represent human disease.

Despite the benefits of using SOD1 models, little progress has been translated into clinical practice (Benatar, 2007), which has led researchers to begin to question what may be missing in the high copy SOD1 mouse model. One limitation of the model is that there is no compound effect of aging with changes occurring so early in life. ALS is a disease that typically

presents in older adulthood, while P90 in mice correlates to younger adulthood. This is important because age-related changes selectively target the same nerve and muscles fibers as ALS (Valdez et al., 2012). This overlap between normal aging and ALS suggests the possibility of similarities in either mechanisms of disease or in compensatory mechanisms to resist disease. These mechanisms interact with each other, furthering disease progression in a way that can simply not be replicated in the high copy SOD1 model. Additionally, this model has substantial overexpression of mutated SOD1 protein, which may cause pathology regardless of mutation (Jaarsma et al., 2000). This has led to some researchers choosing to use a low copy version of the SOD1 mouse model (Del Canto and Gurney, 1997). This model still shows early changes in motor neurons around P10 (Pambo-Pambo et al. 2010) and early cell loss (Acevedo-Arozena et al. 2011); however, symptom onset does not occur until around P230 (Takeuchi et al. 2010). Because these mice are at a stage where some age-related biomarkers begin changing (Flurkey et al., 2007) and do not have as excessive overexpression of SOD1, these mice may better reflect the human condition; however, it is interesting that there are still such early changes.

A third mouse model of interest in this study involves an entirely different genetic approach. This mouse model develops accumulations of TDP43 in the cytoplasm before developing clinical symptoms that resemble ALS in humans. TDP43 is an important regulator of transcription in the central nervous system and, as such, is normally located in the nucleus (Sephton et al., 2014). In most patients with ALS (as well as in those with frontotemporal dementia), however, there is mislocalization, which likely occurs due to mechanisms relating to cell stress, into intracytoplasmic inclusions and thus loss of function of the protein, even without a specific mutation (Da Cruz and Cleaveland, 2011). The substantial number of patients with these inclusions, including in sporadic disease, has led to this protein becoming of considerable interest to researchers, as well this may be a point of convergence across different specific

pathologies, as many pathways that can be involved in familial ALS. Despite the fact that approximately 97% of ALS patients have this accumulation (Lomen-Hoeth et al., 2002), humans (Mackenzie et al., 2007) and mice (Robertson et al., 2008) with SOD1 mutations, however, lack these inclusions, further creating a need to study TDP43 models specifically.

Modeling a loss of function of TDP43 in the mouse, however, comes with significant challenges. Simply knocking out the protein entirely is embryonically lethal, and a heterozygous knockdown causes weakness but no specific motor neuron pathology (Kreamer et al., 2010). This has led to most researchers modeling TDP43 abnormalities with promotors that allow for a knockdown later in development (Reviewed in Wegorzewska and Baloh, 2011). Another strategy is to induce mislocalization of TDP43 later in development by altering the nuclear localization sequence, which causes TDP43 to accumulate in the cytoplasm, which, while not a knockdown, causes a functional loss of protein (Cascella et al. 2016). This can also be made inducible to allow for disease onset to be controlled by something such as the administration of a tetracycline antibiotic such as doxycycline. The experiments herein use a doxycycline-controlled induction of changes to the nuclear localization sequence of TDP43, specifically in the brain and spinal cord (Walker et al., 2015). These mice develop symptoms and death similar to that of the SOD1 mouse models of ALS, provided that they are not returned to doxycycline treatment.

In order to better understand early disease changes in a way that may be more reflective of a disease as opposed to a particular mouse model, this study compares the responses of the sacral spinal reflex circuit in multiple mouse models at the times of early disease changes. While this circuit does not have a direct clinical correlate, this could potentially translate to measures such as an H reflex. The mouse models chosen are the high copy SOD1 mouse model, which is considered a gold standard in ALS research, and the low copy SOD1 model, as this is a more clinically relevant SOD1 model. A mouse model using doxycycline

induced TDP43 mislocalization in the spinal cord, to model an important pathology of all forms of ALS. Experiments are done at the earliest reported time point of disease changes. To further investigate differences between the TDP43 model to the SOD1 models, an adult SOD1 time point was also compared to help determine if differences were developmental or due to model differences.

Hypothesis

The reflex circuit of three different mouse models of ALS are compared at early disease states using electrophysiology. Previous literature using intracellular recordings of motor neurons suggests that motor neurons are hyper-excitable in SOD1 motor neurons at early preclinical time points. Therefore, we hypothesized that there will be evidence of hyperexcitability, such as increased compound action potential amplitudes, and increased response counts to a train of stimuli. While there is no literature on electrophysiological changes early in the disease course for the TDP43 model discussed here, we hypothesize that similar hyperexcitability data will be recorded from this model.

Materials and Methods

Animals

Animals were bred in-house and housed in the Wright State University vivarium. All maintenance and protocols were approved by the Wright State University Animal Care and Use Committee. Three different animal models were used for these experiments, and genotyping was done by tail clipping and analyzed by Transnetyx. Male mice were chosen for all experiments as there are well-documented sex differences in both humans and mice with ALS. The first model is hereafter referred to as the high copy SOD1 model (Gurney et al. 1994), is a transgenic mouse model which over expressed human mutated (G93A mutation) SOD1. These mice were bred in-house from a colony originally purchased from Jackson Laboratories. Females used in these matings did not carry the transgenic genes; however, the males were hemizygous for (Tg(SOD1∗G93A)1Gur) (Stock number 002726). The males express approximately 25 copies of the human G93A mutation of SOD1, which is known to cause ALS, and the offspring which inherit this mutation are referred to as high copy SOD1, while the littermates, which do not are used as control animals, denoted as wild type. Several non-experimental animals were weighed at multiple times prior to weaning (Figure 1). For electrophysiology experiments these mice were used at two different timepoints p (postnatal day) 9-11 (referred to as the P10 time point), chosen because p10 is the earliest time point with recorded cellular changes and p85-95 (p90), which is the time of symptom onset, used in this study as a comparative adult time point. A narrower window is used for the P10 group as this group is experiencing rapid development in its spinal cord and ability to weight bear, as opposed to the P90 group, which is approaching a less tightly controlled time of symptom onset. The second mouse model, hereafter referred to as low copy SOD1, harbors the same transgene and was bred the same way, the only difference

being that these mice only have approximately eight copies of the SOD1 G93A mutation (stock number 032166) (Del Canto and Gurney., 1997).

The third mouse model examined in this study is entirely different. This is a model designed to develop human TDP43 accumulations in the spinal cord using an inducible nuclear mislocalization sequence (Walker et al., 2015). The inducible mutation is suppressed by the administration of doxycycline in the feed. When given doxycycline, these animals do not express the nuclear mislocalization sequence, so no TDP43 accumulates. When doxycycline is no longer administered, cellular changes begin rapidly, and the disease progresses rapidly unless doxycycline administration is resumed. In this experiment, mice were bred in-house using two steps. First, B6C3F1/J (stock number 100010), the background strain, was crossed with NEFH-tTA (stock number 025397) to create heterozygotes with neural expression of a tetracycline antibiotic activator gene. The background strain was also crossed with tetO-TARDP (stock number 014650) to create the offspring with inducible TDP43 mislocalization. Heterozygous offspring from both pairings were then mated. The resulting pups were then genotyped by Transnetyx, and doxycycline was fed first to the mother upon mating and then to the pups when they were old enough to consume solids (Doxycycline Hyclate Diet, Envigo) until P46 (P41-51) when doxycycline was removed for experimental animals. Animals used as controls had the full genetic mutation; however, they remained on doxycycline until the day of the experiment, while experimental animals were placed on regular (without doxycycline feed) exactly seven days before the experiment. This time point was chosen to compare the p10 time points in the SOD1 models as it is the time of the first noted cellular change in this model (Walker et al., 2015).

In Vitro Preparation

Pups

Pups were bred in-house as described above and kept with their mother and littermates until reaching postnatal day 9-11 (the time point of the first reported cellular changes in literature). Animals were first anesthetized with Euthasol solution (150 mg/kg) and allowed to rest (with additional anesthesia given as needed) until the loss of the toe pinch reflex. At this time, animals were surgically decapitated, and the spinal column was removed and placed in mACSF bubbled with 95% oxygen and 5% carbon dioxide. This solution (Bennett et al. 2001) contained the following: 118 mM NaCl, 3 mM KCl, 1.3 mm MgSO4, 5 mM MgCl2, 1.4 mM NaH2PO4, 1.5 mM CaCl2, 24 mM NaHCO3, and 25 mM glucose. The spinal cord was then removed from L4 to CO2 with a ventral laminectomy and placed in a custom-built recording chamber with nACSF. The nACSF (Jiang and Heckman, 2006) was made of the following: 128 mM NaCl, 3 mM KCl, 1.5 mM MgSO4, 1 mM NaH2PO4, 2.5 mM CaCl2, 22 mM NaHCO3, and 12 mM glucose. L5 – S3 ventral roots were mounted on three sets of bipolar electrodes, and the dorsal roots were mounted on a separate set of bipolar electrodes. These were then covered in petroleum jelly to prevent drying and recorded in groups, as seen in Table 1. Data was primarily collected from the S2 and/or S3 ventral roots.

Adults

Adult experiments were also done with animals bred in-house; however, these were weaned and housed with littermates until adult-use time points for the SOD1 high copy or until removal of doxycycline feed, if applicable. These animals then were anesthetized with urethane (0.18 /100 g) until the loss of the toe pinch reflex. They were then given oxygen through a facemask, and the dorsal skin and musculature were removed. A dorsal laminectomy was performed with an oxygenated mACSF drip on the exposed spinal tissue. Once opened, the dura was removed, and the spinal cord and roots was removed from L5 to CO2. This was then placed

in the custom recording chamber as described previously (but larger) with nACSF and allowed to rest approximately 30 minutes before recording.

Table 1

Model	Age	Sex	N	Drug
High Copy SOD1	p9-p11	Male	20	Euthasol
High Copy SOD1	P85-p95	Male	10	Urethane
Low Copy SOD1	P9-p11	Male	6	Euthasol
TDP43	P41-p51	Male	8	Urethane

Table 1 – Experimental groups

Each model discussed herein is listed with important experimental variables. Ages, the drug used for anesthesia, and animal sex are described as these variables may affect the experimental outcome. The sample size for each model is also listed.

Root Data Collection and Analysis

Dorsal roots were stimulated using Isoflex (AMPI) stimulators to bipolar electrodes in a custom-built recording chamber. Data from the adult recording chamber was published previously (Mahrous and Elbasiouny, 2017), and a second smaller version with slight modifications was built for the pup experiments. Stimulation was applied at a multiple of the measured threshold value (the minimum amount of current nA to elicit a visible ventral root response), focusing primarily on low stimulation values. The stimulus was a 25 Hz train applied for four seconds, chosen due to the results of modeling pilot data (Abdelaal et al., 2020). The ventral roots were then mounted on a separate set of bipolar electrodes, and the electrical response was amplified by a custom-built amplifier (Kinetic Software). Data were then digitized by a Power1401 CED board and imported into Spike 2.

Analysis was done manually using Spike 2. The cursors feature was used to take direct manual measurements of compound action potential properties, such as width, amplitude

(Figure 2), and latency (Figure 3). Response counts were made by visual inspection of the trace. To count as a response a signal had to meet the following criteria: first, it had to be larger than noise; second, it had to be wider than noise; and, third, it had to be triphasic (exceptions were made for small responses occurring after the response to the first stimulus where the third phase would not realistically be expected to exceed noise). These responses were counted and characterized as monosynaptic (<6 ms from the stimulus) and polysynaptic (>7 ms from the stimulus), as well as by whether they occurred before or after the first five stimuli in the train, as full synaptic depression occurred within these stimuli.

Statistics

All statistical analysis was performed, and graphs were made in Prism (GraphPad). Each data was tested first for normalcy using a Shapiro Wilk test with an alpha level of 0.05. Data sets that were deemed normal via this test were compared using a Welch's correction T-Test as standard deviations are not consistent across data sets. Data sets that were not normal were compared using a Mann-Whitney U Test. Graphs are shown with error bars illustrating the standard deviation of the mean. Power analysis was performed post hoc in GPower (Franz Faul, University of Keil, Germany).

Results

There are no significant differences in response shape or width for any model

In these experiments, trains of 100 stimuli were applied to ex vivo spinal dorsal roots in three separate ALS disease mouse models. These were then assessed for ventral motor reflexive responses. Specific criteria were set to determine a response to ensure consistency in labeling response and assess basic action potential properties. This included that the response is triphasic and had consistent shape across all recording from a given animal, with a larger amplitude than noise and with a larger width than noise or a non-biological electrical stimulus. There was no difference ($p>0.05$, Figure 1) in the root response threshold (minimum amount of current to evoke a visible response) between wild-type and disease animals (data not shown). Additionally, there were no notable qualitative differences between responses. Response width was calculated in Spike 2 and compared to ensure this consistency was maintained ($p>0.05$ for all models, data not shown). This property conferred confidence that data measured herein were biological and not the result of electrical interference.

However, one thing to note is that while there were no qualitative differences in the electrical responses, there were however differences in pup size that may have affected sampling, including limiting blinding of the experimenter. The current setup could not reliably record from animals less than 5 grams. While there were no differences in weights of animals recorded from, there were significant differences in weight at multiple time points across neonatal development (Figure 1). This may contribute to a sampling bias and does in fact contribute to unequal sample sizes, as at P10 wild-type animals were more likely to meet the size requirements for recording. Data shown are significant ($p<0.05$) and at postnatal days 3, 10, and 20 with SOD1 high copy animals (low copy not shown) significantly smaller than their wild-

type littermates. Weights are normalized to the largest animal in the litter as weight is primarily a function of litter size and maternal milk production.

Figure 1

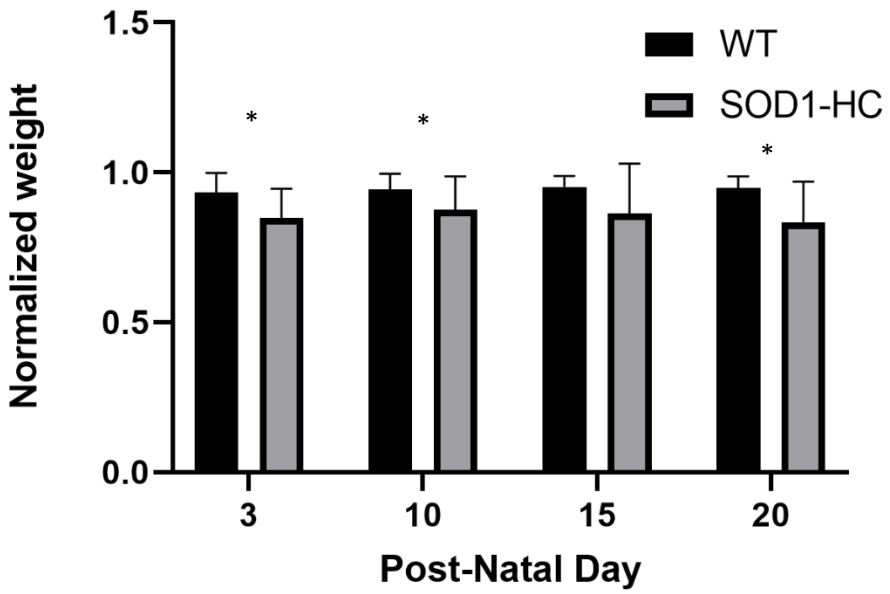

Figure 1 – High copy model weight graph

Animals were measured in grams at four time points across development. They were then normalized to the largest animal in the litter. SOD1 animals are significantly smaller (Wild type N=15, SOD1 N=15 at P3 and P10 and N=10 at P15 and P20; $p<0.05$) at P3 ($P=0.68$), P10 ($P=0.54$), and P20 ($P=0.76$).

Postnatal day 10 mice show significant differences in compound action potential amplitude between mutant and wild type, while adult data does not

To assess the excitability of the spinal circuit, the amplitude of the compound action potential from the ventral root was measured, and each mutant was compared against their respective wild-type animal. Recordings were taken at three different threshold values, and amplitude was measured in millivolts using spike 2 (Figure 2A) and compared with a Welch's T-test or Mann-Whitney U test based on the results of the Shapiro Wilk test for normalcy (see methods for details). Comparisons were made for the responses to each of the first five stimuli in the train separately, as subsequent responses are subject to synaptic depression. Significant results discussed occur at 1.5 times the measured threshold values. In the P10 high copy animals, there was significance in the amplitude of the compound action potential response to the second stimulus ($U<0.05$, Figure 2B). In the P10 low copy animals' significance was found in the first ($U<0.05$, Figure 1c) and second ($U<0.05$, Figure 1c) stimuli. In both instances, SOD1 mutant animals had larger amplitudes than wild-type animals. Significant differences were not seen at any amplitude for the P90 high copy or the TDP43 adult model, however it is of note that the disease animals while insignificantly so were generally smaller than the control animals. Additionally, the absolute value of pup response amplitudes was notably smaller, typically less than one millivolt, while adults typically had responses greater than 1 millivolt even at low amplitude stimulation.

Figure 2

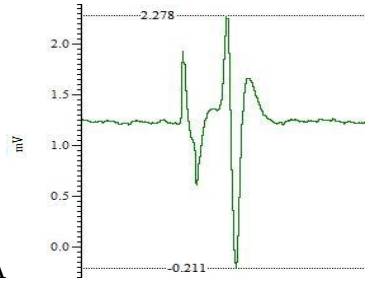

A

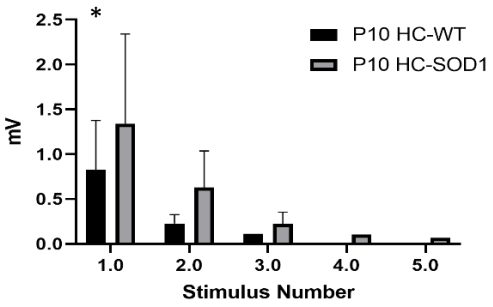

B

WT N=8, n=21
SOD N=6, n=17

C

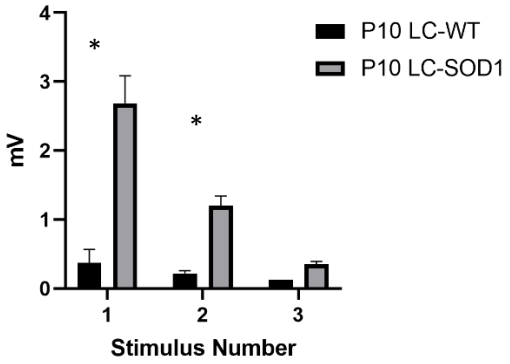

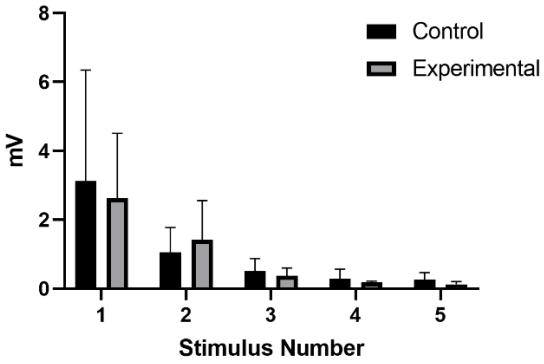

D

WT N=4, n=11
SOD1 N=2, n=6

Control N=7, n=15
Experimental N=3, n=7

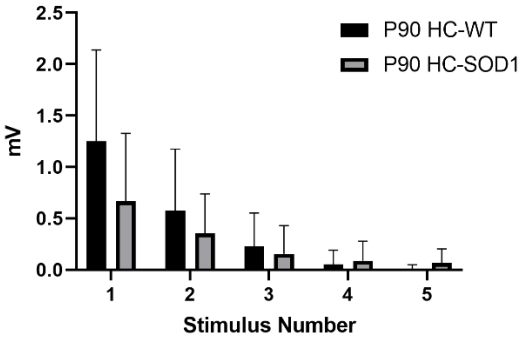

E

WT N=5, n=13
SOD1 N=5, n=12

Figure 2 – Amplitude differences for the first five responses across models

A. An example response with a sampling of how the data was collected. B-E Error bars are standard deviation, N refers to the total number of animals n is the number of root responses. B. P10 high copy WT (N=8, n=21) vs SOD1 (N=6, n=17). Significance occurs in response to the second stimulus ($U<0.05$, $P=0.98$). C. P10 low copy WT (N=4, n=11) vs SOD1 (N=2, n=6). Significance occurs in response to the first and second stimuli ($p<0.05$, $P=1$) D. TDP-43 control (N=7, n=15) vs experimental (N=3, n=7) E. P90 high copy WT (N=5, n=13) vs SOD1 (N=5, n=12).

P10 high copy and TDP-43 mutants show significant differences in early latencies, while low copy and P90 high copy do not

In order to assess the system's kinetics, latency was measured from the onset of the stimulus to the peak of the response, as the peak was the easiest location to determine reliably. Because the width was not different, this is believed to be a reliable choice. Recordings were again taken at three threshold values, and responses are shown at 1.5 times the value for threshold (Figure 2). Latencies were measured in milliseconds using spike 2, and data were normal based on a Shapiro-Wilk Test and were compared using a Welch's T-Test (see methods for more information). Comparisons for each of the first five responses were made separately. P10 high copy showed a significant ($p<0.05$, Figure 2b) difference in response to the first stimulus, whereas TDP43 showed a significant difference in response to the second stimulus ($p<0.05$, Figure2D). P10 low copy and P90 high copy did not show any significance for this measurement. In all models except the low copy (which was insignificant), the disease state had a longer latency than the control animals.

Figure 3

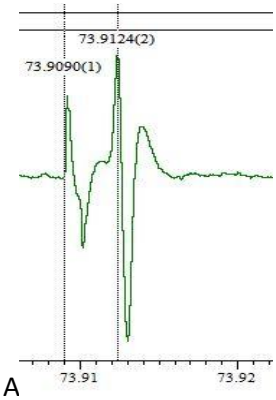

A

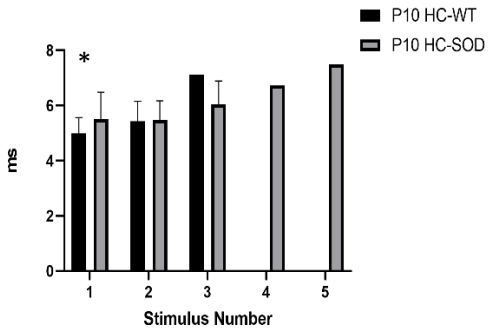

B

WT N=8, n=21
SOD N=6, n=17

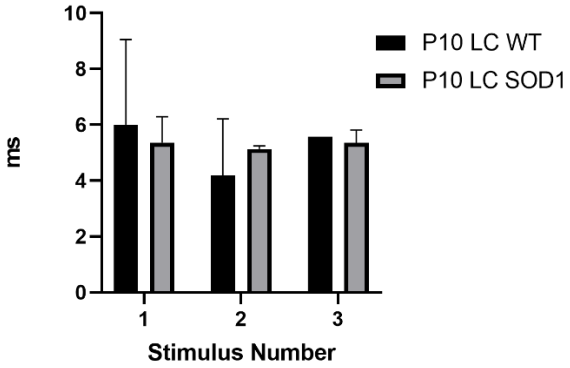

C

WT N=4, n=211
SOD N=2, n=6

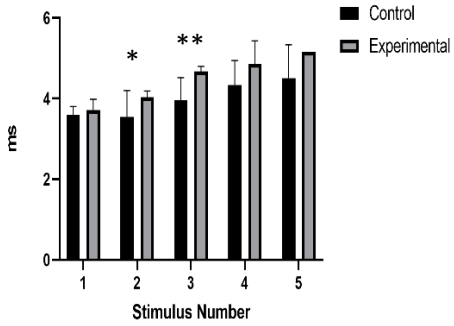

D

Control N=7, n=15
Experimental N=3, n=7

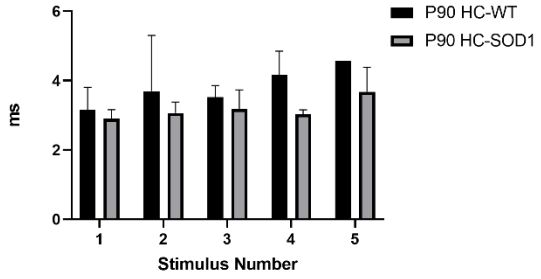

E

WT N=5, n=13
SOD N=5, n=12

Figure 3 –Latency differences for the first five responses across models

A. Illustration of how latency is measured. B-E Error bars are standard deviation B. P10 high copy WT (N=8, n=21) vs SOD1 (N=6, n=17). Significance occurs in response to the first stimulus ($p<0.05$, $P=0.91$). C. P10 low copy WT (N=4, n=11) vs SOD1 (N=2, n=6). Data is insignificant D. TDP-43 control (N=7, n=15) vs experimental (N=3, n=7) Significance occurs in response to the second ($p<0.05$, $P=0.57$) and third stimuli ($p<0.005$, $P=0.95$) E. P90 high copy WT (N=5, n=13) vs SOD1 (N=5, n=12).

All models show differences in the total number of monosynaptic responses

In order to examine a more physiologically relevant parameter of the circuit, trains of 100 stimuli at 25 Hz were applied to the dorsal root, and the number of ventral responses was manually counted (see methods for criteria determining a response). These data are separated by threshold value. Number of animals are reported separately for each threshold value as not all animals were recorded from at every threshold value. These responses were separated into monosynaptic (<6 ms from the stimulus) and polysynaptic (>6 ms from the stimulus) responses as determined by their latency. No significance was found in the number of polysynaptic responses (data not shown). However, the monosynaptic response count showed differences at or approaching significance for at least one threshold value in all models and time points. The P10 high copy model SOD1 showed differences at three times threshold ($p=0.05$, Figure 4B) while the same model at P90 showed differences ($p<0.05$, Figure 4E) at 1.5 times threshold while the low copy SOD1 only had differences at ten times threshold (however with very low

numbers of animals) (Figure 4C). In all three of these SOD1 models, SOD1 animals had a larger response count compared to wild-type animals. Interestingly, in the TDP43 model, the animals on doxycycline had larger response counts than those off doxycycline; this approached significance at 1.5 times the threshold ($p=0.07$, Figure 4E).

Figure 4

A

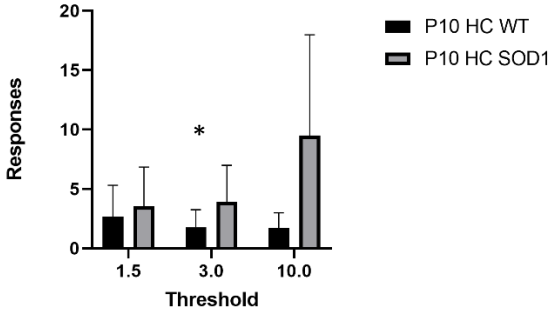

B

N=9 N=5 N=8 N=5 N=4 N=2
n=24 n=15 n=18 n=13 n=11 n=6

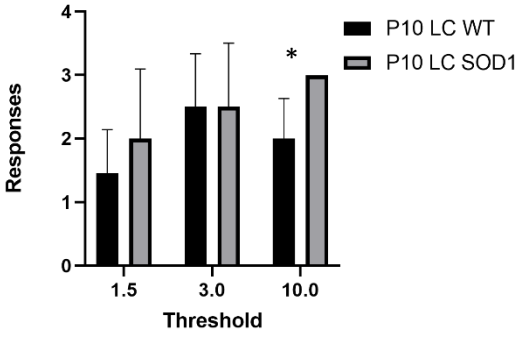

C

N=4 N=2 N=2 N=2 N=2 N=1
n=11 n=6 n=6 n=4 n=6 n=3

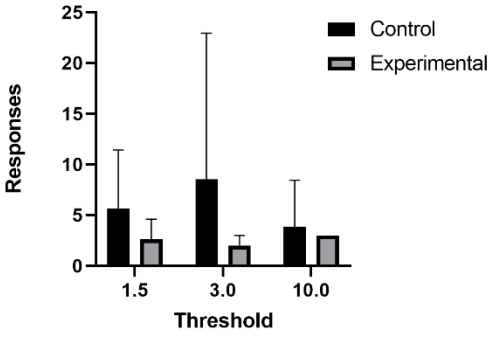

D

N=5 N=3 N=5 N=1 N=5 N=1
n=15 n=8 n=15 n=3 n=14 n=1

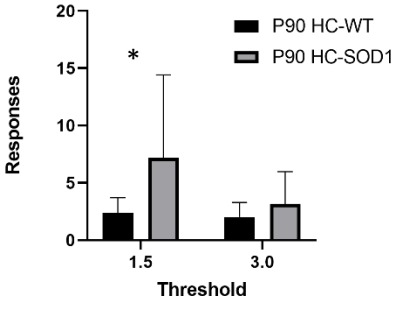

E

N=5 N=5 N=5 N=5
n=13 n=12 n=13 n=11

Figure 4 – Monosynaptic response counts for all amplitudes across models

A. Illustration of how responses are counted. B-E Error bars are standard deviation and significance is noted in p value as all data are normal per the Shapiro Wilks Test. B. P10 high copy WT (1.5T, N=9, n=24, 3T N=8, n=18, 10T N=4, n=11) vs SOD1 (1.5T N=6, n=17, 3T N=5, n =13 10T N=2, n=6). Significance occurs at 3 times threshold (p=0.05, P=0.31). C. P10 low copy WT (1.5T, N=4, n=11, 3T N=2, n=6, 10T N=2, n=6) vs SOD1 (1.5T N=2, n=6, 3T N=2, n =4, 10T N=1, n=3). Data is significant at 10 times threshold ($p<0.05$, P=0.57) D. TDP-43 control (1.5T, N=5, n=15, 3T N=5, n=15, 10T N=5, n=14) vs experimental (1.5T N=3, n=8, 3T N=1, n =3 10T N=1, n=1). Data approaches significance at 1.5 times threshold (p=0.07) E. P90 high copy WT (1.5T, N=5, n=13, 3T N=5, n=12) vs SOD1 (1.5T N=5, n=13, 3T N=5, n =11). Data is significant at 1.5 times threshold ($p<0.05$, P=0.63)

Differences in response count are most pronounced if examined for responses after initial synaptic depression

To further investigate potential causes for these differences in response count, stimulus trains were examined for different synaptic properties, such as maintaining synaptic depression. To do this, the responses that occurred prior to the initial synaptic depression (which typically occurred within the first five stimuli) were subtracted from the total response count. This was then divided by the total to determine what percentage of responses occurred after the initial synaptic depression. This was significant in the threshold values with different monosynaptic counts, except for the low copy SOD1 model, which has an extremely limited sample size. In the P10 high copy at three times the threshold, it was highly significant ($p<0.005$, Figure 5B), as well as the P90 high copy ($p<0.01$, Figure 5E). Additionally, while the TDP43 model had only approached significance ($p=0.07$, Figure 4D) for total response counts in the TDP43 model at 1.5 times the threshold, the response percent was highly significant ($p<0.005$, Figure 5D). However, like with response count, the directionality of significance was different, with the control group on doxycycline showing a higher response percent.

Figure 5

A

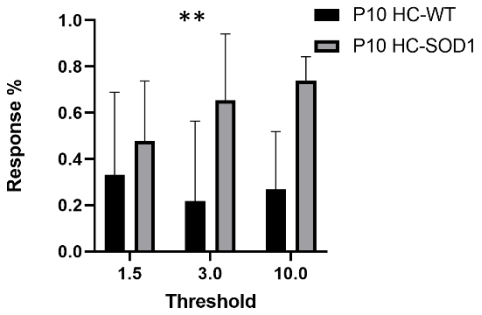

B

N=9 N=5 N=8 N=5 N=4 N=2
n=24 n=15 n=18 n=13 n=11 n=6

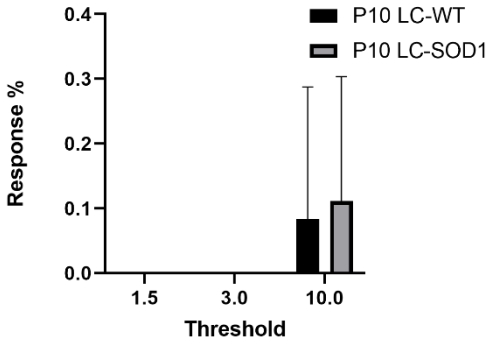

C

N=4 N=2 N=2 N=2 N=2 N=1
n=11 n=6 n=6 n=4 n=6 n=3

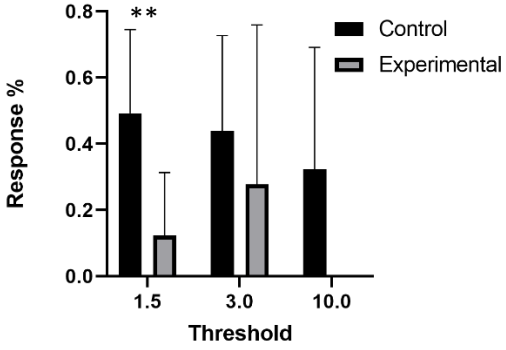

D

N=5 N=3 N=5 N=1 N=5 N=1
n=15 n=8 n=15 n=3 n=14 n=1

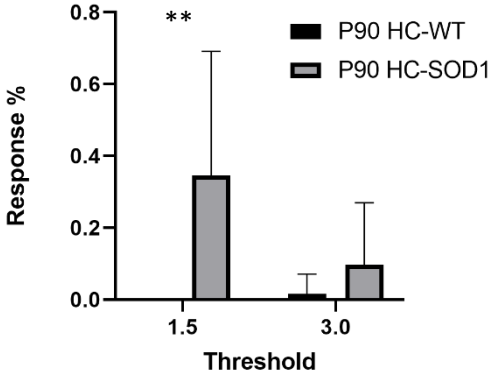

E

N=5 N=5 N=5 N=5
n=13 n=12 n=13 n=11

Figure 5 – Response percentages for all amplitudes across models

A. Illustration of a response occurring after the initial synaptic depression B-E Error bars are standard deviation and significance is noted in p value as all data are normal per the Shapiro Wilks Test. B. P10 high copy WT (1.5T, N=9, n=24, 3T N=8, n=18, 10T N=4, n=11) vs SOD1 (1.5T N=6, n=17, 3T N=5, n =13 10T N=2, n=6). Significance occurs at 3 times threshold ($p<0.01$, $P=0.96$) and at 10 times threshold ($p<0.001$, $P=0.99$). C. P10 low copy WT (1.5T, N=4, n=11, 3T N=2, n=6, 10T N=2, n=6) vs SOD1 (1.5T N=2, n=6, 3T N=2, n =4, 10T N=1, n=3). Data is not significant D. TDP-43 control (1.5T, N=5, n=15, 3T N=5, n=15, 10T N=5, n=14) vs experimental (1.5T N=3, n=8, 3T N=1, n =3 10T N=1, n=1). Data is significant at 1.5 times threshold ($p<0.01$, $P=0.9$) E. P90 high copy WT (1.5T, N=5, n=13, 3T N=5, n=12) vs SOD1 (1.5T N=5, n=13, 3T N=5, n =11). Data is significant at 1.5 times threshold ($p<0.01$, $P=0.94$).

Table 2

Model	**Parameter**			
	Amplitude	*Latency*	*Response Counts*	*Response Percent*
P10 High Copy	Stim 2 $p<0.05$	Stim 2 $p<0.05$	3T $p=0.05$	3T $p<0.01$
P10 Low Copy	Stim 1 and 3 $p<0.05$	NS	10T $p<0.05$	NS
TDP43	NS	Stim 2 $p<0.05$	1.5T $p=0.07$	1.5T $p<0.01$
P90 High Copy	NS	NS	1.5T $p<0.05$	1.5T $p<0.01$

Table 2 – Summary of significance

This table summarizes all significant results presented herein.

Discussion

The experiments described here aim to compare and contrast a reflex spinal circuit of different mouse models of ALS. This was done using dorsal root stimulation in an ex vivo mouse spinal cord preparation and recording the resulting compound action potential from the ventral roots. These data were collected in response to a train of 100 stimuli. This was a stimulation protocol that achieved significance in a modeling study examining P10 SOD1 mice (Abdelaal et al. 2020) for three separate ALS mouse models. The goal was to identify biomarkers that may be used across models as a more reliable indication of disease changes.

Compound Action Potential Properties

Previous literature suggests hyperexcitability in motor neurons at early disease time points (van Dundert et al., 2008; Quinlin et al., 2011; Leroy et al., 2014). However, there is little literature studying the excitability of the whole spinal circuit at early disease stages, even though this may translate to more accessible clinical biomarkers compared to individual cells. To assess excitability in the monosynaptic circuit between the dorsal to ventral spinal roots, we stimulated the dorsal roots and recorded the resulting compound action potential from the ventral root. The ventral root response to the first five stimuli in a stimulus train was analyzed for several different parameters. Unlike in the modeling work, long trains of multiple stimuli fatigued the synapse and created synaptic depression within the first five stimuli.

The first thing analyzed was compound action potential amplitude. This reflects overall excitability in the circuit (Jaing et al., 2017; Mahrous and Elbasiouny, 2017). While less is known about the excitability of dorsal roots, it was hypothesized that because the motor neurons are known to be hyper-excitable in the early disease state for SOD1, these models would show an increased compound action potential amplitude at low amplitude stimulation as more motor

neurons would respond. Amplitude was measured in Spike 2. Both the P10 high copy and P10 low copy showed significantly higher responses in the disease animals. This supports the hypothesis that there would be increased response amplitude because the motor neurons are hyperexcitable. In the high copy model, this difference was more evident in response to the second stimulus in the train, meaning there was a decreased amount of synaptic depression. It is not surprising that results were not significant at the P90 time point in the SOD1 model. This is when disease symptoms emerge and may represent a transition point between hyper and hypoexcitability (Draper, 2021), leading to no net difference. Interestingly, there was also no difference in the TDP43 mouse at early disease stages. Little is currently known about excitability in this model. It is, however, interesting to note that while amplitudes were larger at 1.5 times the threshold, the threshold itself was not different.

Another measured parameter of the initial responses was the latency from stimulus to response. This was measured in Spike 2, as shown in Figure 3A. The peak of the compound action potential was chosen as it was easier to identify reliably than the beginning of the compound action potential when there was a small signal-to-noise ratio. The reliability of this measurement method was confirmed by there being no differences in compound action potential width. Therefore, it is unlikely that differences in latency can be explained by differences in features such as the rate of rise of the action potential. The P10 high copy and the TDP43 model showed differences in this measurement. The disease state had a longer latency than the wild-type animals for significant both models, as well as in the adult high copy model. The modeling data also showed this significance and directionality (Abdelaal et al., 2020) when the model increased cell size. This increased cell size has been reported previously in both the high and low copy SOD1 models at P10 (Dukkipati et al., 2018; Amendola and Durand, 2008) and is consistent with the literature. The P90 high copy motor neurons are not significantly different

in size compared to the wildtype (Dukkipati et al., 2018), and did not have a significant difference in latency. It is not known if TDP43 cells are also larger at this time point. Another factor that plays into this could be that because measurements were taken from the action potential peak, and the peak was higher in P10 high copy SOD1 animals. This could contribute to this difference; however, the difference in amplitude was in response to the second stimulus and not the first, as in the latency. Another factor contributing to this difference could be that perhaps in early disease animals with hyperexcitable motor neurons, more and potentially slower neurons were recruited. Still, more work would need to be done to confirm this hypothesis.

Train Properties

To further study the ALS disease circuitry, the focus was shifted to studying responses to a long train of stimuli. This allowed the study of synaptic properties, such as how many stimuli until the synaptic depression is achieved and how long it is maintained if the stimulus train is continued. One hypothesis for the pathophysiology of ALS is that excess glutamate is released or maintained in the synapse leading to hyper-excitability (Blasco et al., 2014). An alternate hypothesis is that decreased inhibition from inhibitory interneurons contributes to circuit hyperexcitability. Taken together, this led to the hypothesis that there may be an increased number of responses to a long train of stimuli. Responses were categorized as monosynaptic (<6 ms latency) and polysynaptic (>6 ms latency) by their implied mechanism and analyzed separately. Polysynaptic response counts were not significantly different (data not shown). This does not support a difference in interneuron inhibition in this data set. However, monosynaptic response counts were at or close to significance for all models and time points studied. For all the SOD1-based experiments, SOD1 animals had a higher response count than wild-type animals. In the TDP43 animals, the animals off doxycycline had smaller response counts than

wild-type animals. This supports the hypothesis that there is evidence of hyper-excitability in the synapse for SOD1 mouse models, but further investigation would need to be done to better understand the possible difference in the TDP43 model, as these results are likely due to differences in the models as opposed to differences in development.

To further investigate where the differences in response count were coming from, responses were separated as part of the initial set of responses (before any synaptic depression) and after the synaptic depression. This is displayed in figure 5 as a percentage of responses occurring after depression. Interestingly, this data is significant for all groups except the P10 low copy in which significant monosynaptic response counts were seen. The level of significance was also notably higher for many measurements. Like with response counts, this spontaneous return of responses occurred more frequently in the SOD1 disease animals but less frequently in the TDP43 disease animals.

The exact cause for this difference cannot be determined with the current data sets; however, it can be speculated with current literature. Synaptic depression is believed to be caused by neurotransmitter depletion in the synapse (Purves et al., 2019). Typically, repletion does not occur until a period of rest. In the SOD1 animals, it appears as if some change causes repletion to occur before the removal of the stimulus train, while the opposite was true for TDP43. The SOD1 neuromuscular junction is well studied and known to degenerate later in disease (Murray et al., 2010), but significantly less is known potential changes in other synapses. It has also been suggested that SOD1 animals show significant abnormalities in glutamate handling (reviewed in Heath et al. 2002), such as decreased reuptake and abnormalities in proteins tasks with glutamate transport. These abnormalities could allow more glutamate to remain in the synaptic cleft causing this post-depression response. It is also possible, and likely, that these changes reflect some more complex changes in the spinal cord network. These

changes are not a reflection of the serotoninergic inputs as these are not yet developed in the P10 mice (Smith and Brownstone, 2020), however could reflect changes in intraneuronal input. One important synapse of note is the c-bouton, a cholinergic synapse an important role in the neuromodulation, which has been known to be disrupted in ALS, though it's exact role in disease pathogenesis is controversial (Landoni et al., 2019; Konsolaki et al. 2020). It is therefore possible that altered intraneuronal network modulation contributes to this change in synaptic depression maintenance.

Limitations

The first major limitation of this study was the number of animals examined, particularly for the P10 low copy animals. This occurred for several reasons, primarily the variation in animal size observed at this time point. The experimental setup was optimized to the average size of the P10 mice in the given colonies; however, as the animal size is rapidly changing, they could easily be much smaller depending on litter size. Litters were often culled to attempt to prevent this effect, but this was not done until an older age in the low copy strain as opposed to the high copy strain, leading to smaller animals. Additionally, as the weight graph (Figure 1) shows, SOD1 animals are significantly smaller than wild-type animals, impeding collection by making it challenging to collect even groups. TDP43 and low copy SOD1 data collection was also limited by the coronavirus 2019 pandemic. Despite this limitation that prevented the collection of the desired group size, effect size for this data set was surprisingly large, and for the response precent analysis (the most novel finding in this study), a post hoc power analysis was satisfactory with power values greater than or equal to 0.9.

A second major limitation was measurement at different developmental stages. The pups used in this experiment were just beginning to weight bear at this stage, and not all of the

spinal neuronal circuitry was developed yet, and response amplitude was overall much smaller than in the adults. Mice were only just beginning to weight bear and descending spinal inputs do not all reach the sacral cord used in this study (Smith and Brownstone 2020). This made data collection less reliable and limited the ability for direct comparison to the adult-onset models, such as the TDP43 model. To minimize the effect of this limitation, data was collected at an adult time point in the P90 high copy animals. While not at the same disease state (limiting this comparison's ability), it adds validity to the conclusions herein that the models are dramatically different, as opposed to results being due to a developmental difference. The directionality of changes was the same in all SOD1 models, including the P90 high copy (even if insignificant) (SOD1 had larger amplitudes, longer latencies, and more responses after the synaptic depression), leading to the belief that differences in mouse development do not explain the model differences.

Future Directions

This study showed differences across different mouse models for ALS. However, the data herein are inconclusive as to the mechanism for these differences. Further studies, first and foremost, need to be conducted to better understand basic cellular properties in the TDP43 model. To date, there is little published data on excitability changes that could help explain any differences seen, so further work recording basic cell properties of motor neurons in this model is needed.

Additionally, the most interesting finding of this work was the changes to the maintenance of synaptic depression in response to a long train of stimuli. While there is extensive single-cell data on the SOD1 mouse model, less is known about differences at the network level. Examining these differences using a technique such as multi-electrode arrays that

allows for more separation of different cell types would be beneficial to understand better if the fact that the disease affects different types of motor neurons at different rates influenced the results. Lastly, to examine if the changes described herein could be translatable for use in diagnostics for human disease because most of the results described herein occurred at low stimulation values, one could examine changes in similar parameters in H-reflex testing of an accessible human spinal circuit.

Conclusions

This study aimed to compare and contrast early changes in several ALS mouse models to find early biomarkers that may lead to translational testing for patients. An ex vivo model of a reflex circuit was used. These data show significant differences in basic properties of compound action potentials (amplitude and latency) that are consistent with previous literature on hyper excitability and cell size, and properties of long trains, which are a novel finding in this work. These differences, however, were in different directionalities between the SOD1-based models and the TDP43 model, raising questions about possible differences in electrophysiological properties between models. Data described herein is limited; however, it raises questions that warrant further investigation of the similarities and differences between ALS mouse models.

References

1. Abdelaal, Amr Y., et al. "A Classification Approach to Recognize the Firing of Spinal Motoneurons in Amyotrophic Lateral Sclerosis." *2020 42nd Annual International Conference of the IEEE Engineering in Medicine & Biology Society (EMBC)*. IEEE, 2020.
2. Acevedo-Arozena, A., Kalmar, B., Essa, S., Ricketts, T., Joyce, P., Kent, R., ... & Thorpe, J. R. (2011). A comprehensive assessment of the SOD1G93A low-copy transgenic mouse, which models human amyotrophic lateral sclerosis. *Disease models & mechanisms*, dmm-007237.
3. Amendola, Julien, and Jacques Durand. "Morphological differences between wild-type and transgenic superoxide dismutase 1 lumbar motoneurons in postnatal mice." *Journal of Comparative Neurology* 511.3 (2008): 329-341.
4. Arthur, Karissa C., et al. "Projected increase in amyotrophic lateral sclerosis from 2015 to 2040." *Nature communications* 7.1 (2016): 1-6.
5. Benatar, Michael. "Lost in translation: treatment trials in the SOD1 mouse and in human ALS." *Neurobiology of disease* 26.1 (2007): 1-13.
6. Bennett DJ, Li Y, Siu M. Plateau potentials in sacrocaudal motoneurons of chronic spinal rats, recorded in vitro. J Neurophysiol 86 (2001): 1955–1971.
7. Blasco, Hélène, et al. "The glutamate hypothesis in ALS: pathophysiology and drug development." *Current medicinal chemistry* 21.31 (2014): 3551-3575.
8. Boylan, Kevin. "Familial amyotrophic lateral sclerosis." *Neurologic clinics* 33.4 (2015): 807-830.
9. Bryson, Harriet M., Bret Fulton, and Paul Benfield. "Riluzole." *Drugs* 52.4 (1996): 549-563.

10. de Carvalho, Mamede, and Michael Swash. "Lower motor neuron dysfunction in ALS." *Clinical Neurophysiology* 127.7 (2016): 2670-2681.
11. Cascella, Roberta, et al. "Quantification of the Relative Contributions of Loss-of-function and Gain-of-function Mechanisms in TAR DNA-binding Protein 43 (TDP-43) Proteinopathies." *Journal of Biological Chemistry* 291.37 (2016): 19437-19448.
12. Da Cruz, Sandrine, and Don W. Cleveland. "Understanding the role of TDP-43 and FUS/TLS in ALS and beyond." *Current opinion in neurobiology* 21.6 (2011): 904-919.
13. Dal Canto, M. C., & Gurney, M. E. (1997). A low expressor line of transgenic mice carrying a mutant human Cu, Zn superoxide dismutase (SOD1) gene develops pathological changes that most closely resemble those in human amyotrophic lateral sclerosis. *Acta neuropathologica*, *93*(6), 537-550.
14. Draper, C. S.I. (2021). *ALS-induced Excitability Changes in Individual Motorneurons and the Spinal Motorneuron Network in SOD1-G93A Mice at Symptom Onset* [Doctoral dissertation, Wright State University]. OhioLINK Electronic Theses and Dissertations Center.
15. Dukkipati, S. Shekar, Teresa L. Garrett, and Sherif M. Elbasiouny. "The vulnerability of spinal motoneurons and soma size plasticity in a mouse model of amyotrophic lateral sclerosis." *The Journal of physiology* 596.9 (2018): 1723-1745.
16. Genç, B. *et al.* Apical dendrite degeneration, a novel cellular pathology for Betz cells in ALS. *Sci. Rep.* **7**, 41765; doi: 10.1038/srep41765 (2017).
17. Gurney, Mark E., et al. "Motor neuron degeneration in mice that express a human Cu, Zn superoxide dismutase mutation." *Science* 264.5166 (1994): 1772-1775.

18. Hegedus, J., C. T. Putman, and T. Gordon. "Time course of preferential motor unit loss in the SOD1G93A mouse model of amyotrophic lateral sclerosis." *Neurobiology of disease* 28.2 (2007): 154-164.
19. Jaarsma, Dick, et al. "Human Cu/Zn superoxide dismutase (SOD1) overexpression in mice causes mitochondrial vacuolization, axonal degeneration, and premature motoneuron death and accelerates motoneuron disease in mice expressing a familial amyotrophic lateral sclerosis mutant SOD1." *Neurobiology of disease* 7.6 (2000): 623-643.
20. Jiang MC, Heckman CJ. In vitro sacral cord preparation and motoneuron recording from adult mice. J Neurosci Methods 156 (2006): 31–36.
21. Jiang, Mingchen C., et al. "Hyperexcitability in synaptic and firing activities of spinal motoneurons in an adult mouse model of amyotrophic lateral sclerosis." *Neuroscience* 362 (2017): 33-46.
22. King, Anna E., et al. "Excitotoxicity in ALS: Overstimulation, or overreaction?." *Experimental neurology* 275 (2016): 162-171.
23. Konsolaki, Eleni, et al. "Genetic inactivation of cholinergic C bouton output improves motor performance but not survival in a mouse model of amyotrophic lateral sclerosis." *Neuroscience* 450 (2020): 71-80.
24. Kraemer, Brian C., et al. "Loss of murine TDP-43 disrupts motor function and plays an essential role in embryogenesis." *Acta neuropathologica* 119.4 (2010): 409-419.
25. Kurland, L. T., & Mulder, D. W. (1955). Epidemiologic Investigations of Amyotrophic Lateral Sclerosis: 2. Familial Aggregations Indicative of Dominant Inheritance Part II. *Neurology*, *5*(4), 249-249.

26. Landoni, Lauren M., et al. "Cholinergic modulation of motor neurons through the C-boutons are necessary for the locomotor compensation for severe motor neuron loss during amyotrophic lateral sclerosis disease progression." *Behavioural brain research* 369 (2019): 111914.
27. Leroy, Félix, et al. "Early intrinsic hyperexcitability does not contribute to motoneuron degeneration in amyotrophic lateral sclerosis." *Elife* 3 (2014): e04046.
28. Lomen-Hoerth, Catherine, Thomas Anderson, and Bruce Miller. "The overlap of amyotrophic lateral sclerosis and frontotemporal dementia." *Neurology* 59.7 (2002): 1077-1079.
29. Ludolph, A. C., T. Meyer, and M. W. Riepe. "The role of excitotoxicity in ALS–what is the evidence?." *Journal of neurology* 247.1 (2000): I7-I16.
30. Mackenzie, Ian RA, et al. "Pathological TDP-43 distinguishes sporadic amyotrophic lateral sclerosis from amyotrophic lateral sclerosis with SOD1 mutations." *Annals of Neurology: Official Journal of the American Neurological Association and the Child Neurology Society* 61.5 (2007): 427-434.
31. Mahrous, Amr A., and Sherif M. Elbasiouny. "SK channel inhibition mediates the initiation and amplitude modulation of synchronized burst firing in the spinal cord." *Journal of Neurophysiology* 118.1 (2017): 161-175.
32. Paganoni, Sabrina, et al. "Diagnostic timelines and delays in diagnosing amyotrophic lateral sclerosis (ALS)." *Amyotrophic Lateral Sclerosis and Frontotemporal Degeneration* 15.5-6 (2014): 453-456.
33. Pambo-Pambo AB, Durand J, Gueritaud JP (2009) Early excitability changes in lumbar motoneurons of transgenic SOD1G85R and SOD1G93A-Low mice. J Neurophysiol 102:3627-3642.

34. Purves, D., Augustine, G. J., Fitzpatrick, D., Hall, W., LaMantia, A. S., & White, L. (2019). *Neurosciences*. De Boeck Supérieur.

35. Quinlan, K. A., et al. "Altered postnatal maturation of electrical properties in spinal motoneurons in a mouse model of amyotrophic lateral sclerosis. *The Journal of physiology* 589.9 (2011): 2245-2260.

36. Rosen, Daniel R., et al. "Mutations in Cu/Zn superoxide dismutase gene are associated with familial amyotrophic lateral sclerosis." *Nature* 362.6415 (1993): 59-62.

37. Sephton, Chantelle F., et al. "TDP-43 in central nervous system development and function: clues to TDP-43-associated neurodegeneration." *Biological chemistry* 393.7 (2012): 589-594.

38. Smith, Calvin C., and Robert M. Brownstone. "Spinal motoneuron firing properties mature from rostral to caudal during postnatal development of the mouse." *The Journal of physiology* 598.23 (2020): 5467-5485.

39. Statland, J. M., Barohn, R. J., McVey, A. L., Katz, J. S., & Dimachkie, M. M. (2015). Patterns of Weakness, Classification of Motor Neuron Disease, and Clinical Diagnosis of Sporadic Amyotrophic Lateral Sclerosis. *Neurologic clinics*, *33*(4), 735-48.

40. Swash, M. I. C. H. A. E. L., and D. A. V. I. D. Ingram. "Preclinical and subclinical events in motor neuron disease." *Journal of Neurology, Neurosurgery & Psychiatry* 51.2 (1988): 165-168.

41. Takeuchi, Shigeko, Noriko Fujiwara, Akemi Ido, Miki Oono, Yuki Takeuchi, Minako Tateno, Keiichiro Suzuki et al. "Induction of protective immunity by vaccination with wild-type apo superoxide dismutase 1 in mutant SOD1 transgenic mice." *Journal of Neuropathology & Experimental Neurology*69, no. 10 (2010): 1044-1056.

42. Talbott, Evelyn O., Angela M. Malek, and David Lacomis. "The epidemiology of amyotrophic lateral sclerosis." *Handbook of clinical neurology* 138 (2016): 225-238.
43. van den Bos, Mehdi AJ, et al. "Pathophysiology and diagnosis of ALS: insights from advances in neurophysiological techniques." *International journal of molecular sciences* 20.11 (2019): 2818.
44. Van Zundert, Brigitte, et al. "Neonatal neuronal circuitry shows hyperexcitable disturbance in a mouse model of the adult-onset neurodegenerative disease amyotrophic lateral sclerosis." *Journal of Neuroscience* 28.43 (2008): 10864-10874.
45. Walker, Adam K., et al. "Functional recovery in new mouse models of ALS/FTLD after clearance of pathological cytoplasmic TDP-43." *Acta neuropathologica* 130.5 (2015): 643-660.
46. Wegorzewska, Iga, and Robert H. Baloh. "TDP-43-based animal models of neurodegeneration: new insights into ALS pathology and pathophysiology." *Neurodegenerative Diseases* 8.4 (2011): 262-274.